Broadband All-Optical Ultrasound Transducer

Yang HOU [1], Jin-Sung KIM [1], Shai ASHKENAZI [2], Sheng-Wen HUANG [2],
L. Jay GUO [1], Matthew O'DONNELL [3]

[1] Department of Electrical Engineering and Computer Science, University of Michigan,
Ann Arbor, MI, 48109 USA; yanghou@eecs.umich.edu, jskim@umich.edu, guo@eecs.umich.edu,
Phone: 1-734 6477718, Fax 1-734 7639324
[2] Department of Biomedical Engineering, University of Michigan, Ann Arbor, MI, 48109 USA
shaia@umich.edu, shengwen@umich.edu
[3] Department of Bioengineering, University of Washington, Seattle, WA, 98195 USA
odonnel@engr.washington.edu

Abstract
Real-time three-dimensional (3D) high-resolution ultrasound imaging requires 2D phased arrays
operating at frequencies higher than 50 MHz, which poses a great challenge for piezoelectric
technologies. A promising alternative is an optoacoustic array relying on optical generation and detection
of ultrasound. We present an all-optical ultrasound transducer, which consists of a 2D gold nanostructure
on a glass substrate, topped by a 2.7 µm polydimethylsiloxane (PDMS) layer and then a 30 nm gold layer.
A laser pulse with a wavelength matches that of the surface plasmon resonance of the gold nanostructure
caused the absorption of a large fraction of the incident optical energy and heat a highly localized volume;
and a rapid thermal expansion launches an acoustic wave. The gold nanostructure also reflects over 90%
of optical energy at wavelengths far from the resonance, which, together with the continuous gold layer
and the PDMS bulk in between, forms a Fabry-Perot etalon structure for ultrasound detection. Large
bandwidth (57 MHz) and high resolution are demonstrated by pulse-echo imaging experiments.
Keywords: All-optical ultrasound transducer, optical generation and detection of ultrasound, surface
plasmon resonance, gold nanostructure, Fabry-Perot etalon

1. Introduction

High frequency (> 30 MHz) ultrasound has been widely used in various applications
including ophthalmology [1], intravascular imaging (IVUS) [2] and small animal
imaging [3]. Two-dimensional (2D) transducer arrays are highly desired to make high
quality images of a 3D volume because they can be steered and dynamically focused in
the image plane, and can achieve higher frame rates. However, piezoelectric array
systems are not yet available for routine use at high frequencies despite significant
progress by several investigators [4], where major problems include dicing
piezoceramics to micron scale elements, electrical connections, crosstalk between
elements, as well as lack of quality high frequency materials and electronics. Recently,
the capacitive micromachined ultrasound transducer (CMUT) has been developed as an
alternative [5], but these devices require integrated front-end electronics for each
independent array element. Therefore, for applications where high frequency and
broadband arrays with large element counts are required in simple packages, a new
transduction technology is still greatly needed.

An attractive alternative to conventional piezoelectric technology is an optoacoustic
array relying on optical generation and detection of ultrasound. Two laser beams are
used as input/output instead of electronic signals, one for ultrasound generation and the
other for ultrasound detection. The most significant advantage over piezoelectricity is
that the size and spacing of each transmit/receive array element is defined by the focal

spot of a laser beam, and can be easily reduced to several microns using conventional optics, which is suitable for synthetic aperture imaging at frequencies over 100 MHz. Also, an array can be easily formed by splitting the primary laser beam and focusing the resultant secondary beams onto an array of spots, avoiding the trouble of dicing the transducer surface or making any electrical connections.

The most common and efficient mechanism for optical generation of ultrasound is the thermoelastic effect [6]. Typically, a laser pulse is focused onto the surface of a light-absorbing film, causing a rapid temperature rise in a localized volume, where thermal expansion launches an acoustic wave into the overlying sample. The current state-of-the art optoacoustic transmitter [7] consists of a 2D array of gold nanoparticles as optical absorber and a thin polydimethylsiloxane (PDMS) layer with high thermal expansion coefficient to improve the optoacoustic transduction efficiency. These devices can easily generate acoustic surface pressure exceeding 100 MPa at above 50 MHz, making them proper tools for real-time biomedical imaging applications.

One of the most effective methods for optical detection of ultrasound is to utilize an etalon structure [8], also known as a Fabry-Perot interferometer, which is an optical device that consists of a polymer layer sandwiched between two optical reflectors. Multiple beam interference effect makes an output optical signal highly sensitive to the optical path length near the resonance wavelength. Acoustic waves propagating through the etalon modulates the cavity length, which in turn changes the reflected optical intensity; thus, the acoustic pressure can be measured by recording the intensity change of the reflected signal. Etalon sensitivity has been shown to be comparable to a piezoelectric transducer of equivalent size, and etalon bandwidth can easily exceed 100 MHz with a very thin polymer layer.

Both optoacoustic transmitters and receivers have been significantly improved during the past decade, and are mature enough to be integrated into a single device for practical imaging applications. In this paper, the design and fabrication of an integrated all-optical ultrasound transducer as well as the characterization of the optical and acoustic properties are explored. Images obtained from a 1D synthetic aperture are also presented.

2. Fabrication and Structure

The most crucial part of the device is the 2D gold nanostructure used for generating the acoustic waves. Such 2D Au nanostructure was fabricated by Nanoimprint Lithography and Au evaporation [9]. The mold used for nanoimprinting consists of a 220 nm period 2D SiO_2 pillar array of 200 nm deep and 128 nm by 110 nm in cross section on a Si wafer. Such a pillar structure mold was fabricated by a combination of two-orthogonal imprinting using a 220nm period grating mold, metal mask deposition, and reactive ion etching [10]. Figure 1(a) shows a scanning electron microscope (SEM) picture of the top view of a 20 nm thick gold nanostructure deposited on the imprinted polymer template, and Figure 1(b) shows a sketch of the side view. A mixture of PDMS and D4 is then spin-coated on top of the gold nanostructure, where the thickness is about 2.7 μm. A 30 nm thick gold layer is then deposited in a second gold evaporation. As a final step, an additional 0.5 μm thick PDMS layer is spin cast over the entire device for protection. A sketch of the side view of the entire structure is shown in Figure 1(c).
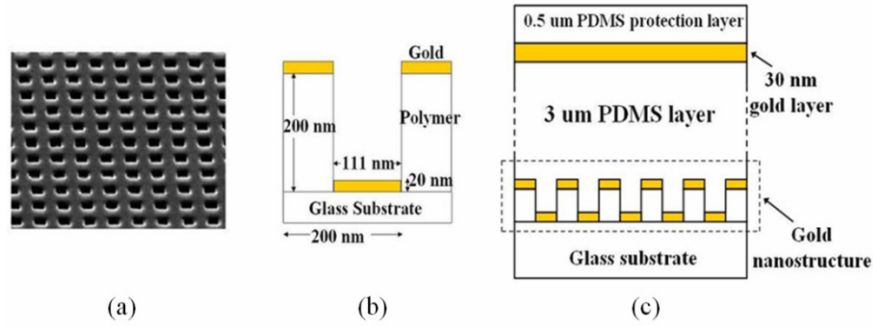
Figure 1. (a) SEM picture of the top view and (b) sketch of the side view of the 2D gold nanostructure; (c) Sketch of the side view of the all-optical transducer structure.

3. Experiment and Results

The gold nanoparticles in the structure serve as efficient optical absorbers because the surface plasmons localized at the particles strongly absorb light at a resonant wavelength, determined to be about 780 nm for our structure. Optical transmission has been measured to be 20% at wavelength of 780 nm and 15% at 1550 nm, while optical reflection from the substrate side of the gold nanostructure is 50% at 780 nm and 75% at 1550 nm. This means that optical extinction, mostly due to optical absorption, is about 30% at 780 nm, and 10% at 1550 nm. As a result, a short laser pulse at 780 nm can be focused onto the gold nanostructure for high-frequency ultrasound generation.

An etalon is formed for optical detection of ultrasound with the gold nanostructure, the additional 30 nm gold layer, and the 2.7 μm PDMS layer in between. A high quality factor is achieved because the optical reflection from the polymer side of the gold nanostructure is measured to be above 85% over 1440 to 1590 nm wavelength. Figure 2(a) shows the optical reflection resonance around 1520 nm with FWHM of 10.5 nm. A high frequency piezoelectric transducer is used to characterize the frequency response of the etalon. The transducer pulse-echo signal reflected from a glass substrate and the etalon signal from detecting the transducer are recorded. Both spectra, together with the derived frequency response of the etalon, are shown in Figure 2(b). Clearly, the etalon is suitable for ultrasound detection exceeding 50 MHz.
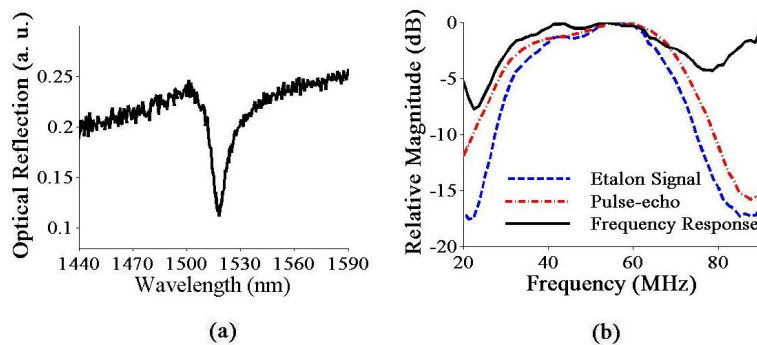
Figure 2. (a) Optical resonance of the etalon structure (b) Spectrum of the etalon signal, the square root of pulse-echo signal of the piezoelectric transducer, and the etalon frequency response (derived by dividing the etalon spectrum by the square root of transducer pulse-echo spectrum).

A simple ultrasound pulse-echo experiment is performed. The detailed setup is described elsewhere [9]. Briefly, the integrated all-optical transducer is mounted at the bottom of a water tank. A 5 ns laser pulse at the wavelength of 780 nm is illuminated and focused onto a 70 μm spot, on the gold nanostructure with energy of about 1

µJ/pulse (fluence of 26 mJ/cm^2). Currently, a 70 µm spot is the minimum diameter for our setup. A continuous-wave (CW) laser beam at 1517 nm with power of 4 mW is used to detect the pulse-echo acoustic waves reflected back from a glass slide aligned parallel to the etalon surface and placed about 1.5 mm away. The beam is illuminated on the etalon, focused onto a concentric 20 µm spot. Reflected light, which has been modulated by the pulse-echo ultrasound waves, is collected using an amplified InGaAs photodiode. The signal is amplified by 30 dB before data capture.

Figure 3(a) shows the pulse-echo signal with 1000 averages. The signal to noise ratio (SNR) of a single-shot signal is measured to be over 10 dB for this experiment in which only a very small fraction of the transmitted acoustic power is captured by the 20 µm diameter receive aperture. The spectrum of the pulse-echo signal (solid curve), averaged 1000 times, is shown in Figure 3(b). The center frequency is 40 MHz, with -6 dB bandwidth of 57 MHz. The theoretical spectrum (dashed curve) is also shown for comparison, which is derived by taking the spectrum of the time derivative of the laser pulse, multiplying it by the etalon frequency response, then taking into account the attenuation in water. Apparently, the two curves are in reasonably good agreement with each other.
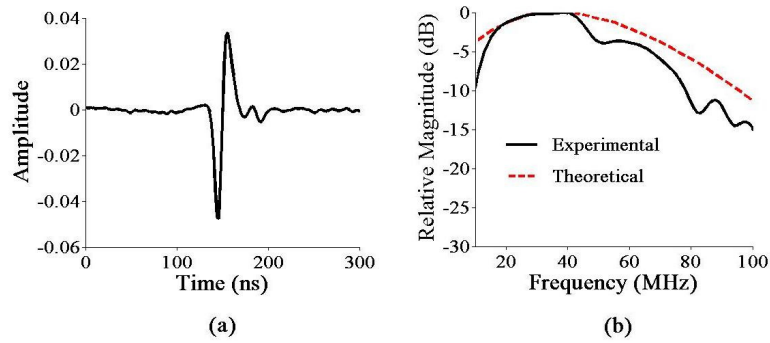
Figure 3. (a) Pulse-echo signal averaged 1000 times, and (b) spectrum of averaged pulse-echo signal compared to simulation results.

To further evaluate this all-optical ultrasound transducer, its ultrasound imaging capabilities must be demonstrated. An imaging object, instead of the glass slide, is placed about 1.5 mm away from the transducer while everything else remains the same. A 1-D synthetic aperture is formed by mechanically scanning the imaging object. A 25 µm diameter metal wire is used as the imaging target, which is scanned over a total distance of 2 mm with 20 µm step separation. At each position, the signal is averaged 100 times before recording. Figure 4(a) shows a wavefield plot of the detected acoustic field. Band-pass filtering (25 to 85 MHz) and demodulation are applied, and then beam forming according to a simple synthetic aperture focusing technique (SAFT) is performed to reconstruct the image, shown in Figure 4(b). The -6 dB axial resolution is determined to be 19 µm, consistent with the bandwidth of the pulse. This also confirms that only the echo from the wire front edge contributes to the image because the axial resolution is smaller than the actual wire diameter. The -6 dB lateral resolution is 38 µm, representing about one acoustic wavelength at the 40 MHz center frequency.
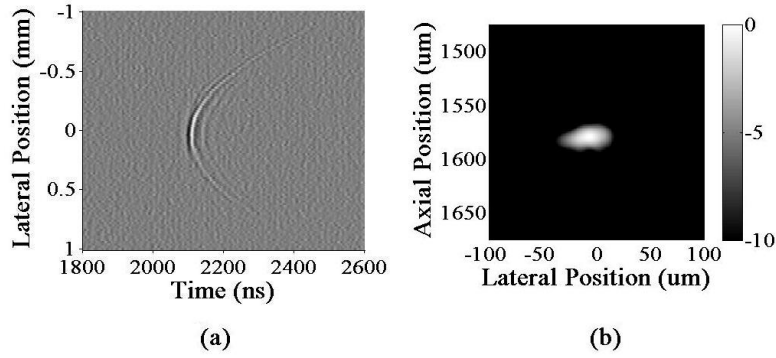
Figure 4. (a) Wavefield plot of the detected acoustic field (b) reconstructed image

4. Discussion

At this stage, the imaging target is mechanically scanned to form an equivalent 1-D synthetic aperture. However, simultaneous detection at all array elements, and even simultaneous excitation in some configurations, is required for real-time imaging applications. This can be realized by splitting both the illumination and detection beams into an array of focused spots on the surface of the device. For laser beam delivery, a graded index (GRIN) fiber bundle can be used, which contains several thousand individual light guides, each having a diameter and spacing of 10 to 20 μm. The small size of each individual light guide provides convenience to achieve smaller element size, which is critical for limiting the divergence of the radiation pattern for high-frequency imaging. Laser power needs to be increased corresponding to the total number of elements used, which can be done using Erbium doped fiber amplifiers (EDFA). The uniformity of the device is important especially for ultrasound detection, because the thickness of the structure determines the optimal wavelength for the detection laser beam. This must be equal to or close to the actual wavelength used at all element spots. Good uniformity is expected after further refinement of current fabrication methods. Meanwhile, InGaAs photodiode arrays are commercially available, which can be integrated into our system with proper modifications for simultaneous detection of multiple probing beams. Therefore, expanding a single element optoacoustic transducer into an array system can be practically done using a splitting and focusing scheme.

Another practical consideration for building an array system is to achieve SNR higher than 10 dB in our current single element system. This requires higher generated acoustic pressure and lower etalon noise equivalent pressure. Such higher acoustic pressure can be efficiently generated by increasing input pulse laser energy. Also, the etalon noise equivalent can be reduced by increasing the probing laser beam intensity, improving etalon quality factor, as well as utilizing photodetectors with higher sensitivity. The acoustic pressure has the potential to be improved by 20 dB simply by increasing the input energy from 1 μJ/pulse to above 10 μJ/pulse, while it is not difficult to reduce the noise equivalent pressure by at least another 20 dB by increasing the probing laser power from 4 mW to 20 mW and the etalon quality factor from 150 to 300. Thus, the SNR of a single shot pulse-echo signal from a single element can easily exceed 50 dB without damaging the device, a value more than sufficient for a 2-D array element.

5. Summary

We have designed, fabricated, and tested the broadband all-optical ultrasound transducer. The pulse-echo signal displays good SNR and excellent bandwidth. High-resolution ultrasound imaging has been demonstrated using a 1D synthetic aperture Planned next steps include optimizing the gold nanostructure for maximal optical absorption at the resonance wavelength, modifying the experimental system to achieve higher SNR, and expanding a single transducer element to an array system for real-time imaging. We believe that these all-optical ultrasound transducers are suitable for 2D high frequency arrays providing real-time 3D high resolution imaging capability.

Acknowledgements

References

1. F. S. Foster, C. J. Pavlin, G. R. Lockwood, L. K. Ryan, K. A. Harasiewicz, L. Berube, and A. M. Rauth, "Principles and applications of ultrasonic backscatter microscopy," *IEEE Trans. Ultrason., Ferroelect., Freq. Contr.*, 40, pp 608–616, 1993.
2. R. A. White, C. E. Donayre, G. E. Kopchock, I. Walot, C. M. Mehinger, E. P. Wilson, and C. de Virgilio, "Vascular imaging before, during and after endovascular repair," *World J. Surg.*, 20, pp 622–629, 1996.
3. D. H. Turnbull, J. A. Ramsay, G. S. Shivji, T. S. Bloomfield, L. From, D. N. Sauder, and F. S. Foster, "Ultrasound backscatter microscope analysis of mouse melanoma progression," *Ultrasound Med. Biol.*, 22, pp. 845–853 1996.
4. K. A. Snook, C. H. Hu, T. R. Shrout, and K. K. Shung, "High-frequency ultrasound annular-array imaging. Part I: Array design and fabrication," *IEEE Trans. Ultrason., Ferroelect., Freq. Contr.*, 53, pp 300–308, 2006.
5. O. Oralkan, S.T. Hansen, B. Bayram, G.G. Yaralioglu, A.S. Ergun, and B.T. Khuri-Yakub, "High-frequency cMUT arrays for high-resolution medical imaging," *Proc. IEEE Ultrason. Symp.*, 1, pp 399–402, 2004.
6. T. Buma, M. Spisar, and M. O'Donnell, "High-frequency ultrasound array element using thermoelastic expansion in an elastomeric film," *Appl. Phys. Lett.*, 79, pp 548–550, 2001.
7. Y. Hou, J. S. Kim, S. Ashkenazi, M. O'Donnell, and L. J. Guo, "Optical generation of high frequency ultrasound using two-dimensional gold nanostructure," *Appl. Phys. Lett.*, 89, 093901, 2006.
8. P. C. Beard and T. N. Mills, "Extrinsic optical-fiber ultrasound sensor using a thin polymer film as a low-finesse Fabry-Perot interferometer," *Appl. Opt.*, 35, pp 663–675, 1996.
9. Y. Hou, J. S. Kim, S. Ashkenazi, S. W. Huang, L. J. Guo, and M. O'Donnell, "Broadband all-optical ultrasound transducers," *Appl. Phys. Lett.*, 97, 073507, 2007.
10. B. D. Lucas, J. Kim, C. Chin and L. J. Guo, "Nanoimprint Lithography Based Approach for the Fabrication of Large-Area, Uniformly-Oriented Plasmonic Arrays", *Adv. Mater.* 20, 1129–1134, 2008.